Plant Physiol. (1983) 71, 810–817
0032-0889/83/71/0810/08/$00.50/0

An Interpretation of Some Whole Plant Water Transport Phenomena

Received for publication August 22, 1982 and in revised form November 30, 1982

EDWIN L. FISCUS, ARNOLD KLUTE, AND MERRILL R. KAUFMANN
United States Department of Agriculture-Agricultural Research Service, Crops Research Laboratory, Colorado State University, Fort Collins, Colorado 80523 (E. L. F.); United States Department of Agriculture-Agricultural Research Service, Agronomy Department, Colorado State University, Fort Collins, Colorado 80523 (A. K.); and United States Department of Agriculture—Forest Service, Rocky Mountain Forest and Range Experiment Station, Fort Collins, Colorado 80526 (M. R. K.)

ABSTRACT

A treatment of water flow into and through plants to the evaporating surface of the leaves is presented. The model is driven by evaporation from the cell wall matrix of the leaves. The adsorptive and pressure components of the cell wall matric potential are analyzed and the continuity between the pressure component and the liquid tension in the xylem established. Continuity of these potential components allows linking of a root transport function, driven by the tension in the xylem, to the leaf water potential. The root component of the overall model allows for the solvent-solute interactions characteristic of a membrane-bound system and discussion of the interactions of environmental variables such as root temperature and soil water potentials. A partition function is developed from data in the literature which describes how water absorbed by the plant might be divided between transpiration and leaf growth over a range of leaf water potentials.

Relationships between the overall system conductance and the conductance coefficients of the various plant parts (roots, xylem, leaf matrix) are established and the influence of each of these discussed.

The whole plant flow model coupled to the partition function is used to simulate several possible relationships between leaf water potential and transpiration rate. The effects of changing some of the partition function coefficients, as well as the root medium water potential on these simulations is illustrated.

In addition to the general usefulness of the model and its ability to describe a wide range of situations, we conclude that the relationships used, dealing with bulk fluid flow, diffusion, and solute transport, are adequate to describe the system and that analogically based theoretical systems, such as the Ohm's law analogy, probably ought to be abandoned for this purpose.

Frequently the question arises about what type of relationship one should expect between leaf water potential (ψ^l), transpiration rate (T), and root medium water potential (ψ^0 for either soil or solution). The most frequently used model is related in some way to the Ohm's law analogy. The most frequently used interpretation of this analogy (correct or not) and therefore the answer to the question raised above is that we should expect a linear relationship between the soil-leaf potential difference and transpiration which passes through the origin. In this paper, we will reexamine this question on an elementary level and show several reasons why such expectations are not necessarily well founded. It is the purpose of this paper to present a model of whole plant water flow, to examine how this model might respond to changes in various parameters, and to settle on whether our expectations based on the Ohm's law analogy are reasonable.

THE MODEL

The simplified plant system schematic is shown in Figure 1. It consists only of a long tube, the xylem, bounded on the left by the "root membrane" and on the right by the leaf matrix from which water evaporates, driving flow through the system, assuming there is a source of water in contact with the root. Obviously, the figure is neither complete nor accurate. The root membrane is shown as a single flat surface. It is in reality cylindrical in nature and is probably made up of several membranes in a series or parallel arrangement with intervening cytoplasm. The xylem is shown as a single tube instead of a collection of branched and unbranched tubes of various sizes and cellular maturities and no adjacent tissue is indicated. The leaf matrix is, similar to the root membrane, shown as a single homogeneous phase when the real geometric complexity must be quite astounding.

A schematic detail of the leaf tissue phase is shown in Figure 2 with arrows indicating the overall direction of flow and possible exchanges with cell protoplasts. The leaf matrix phase of Figure 1 includes only the cell wall phase of the tissue. The pressure (turgor) component of the protoplast phase is distinct from the pressure component of the cell wall matrix phase which will be discussed shortly.

As previously stated, the whole system is driven by evaporation from the leaf matrix. Water then moves through the stomata into the atmosphere. The rate of this process is controlled by the energy gradient from the leaf to the air and the diffusive conductance of the leaf surface (including stomata). We are not presently concerned about the transpirational forces involved here or for that matter what causes the stomata to open and close. Our only interest in the evaporative process is in its rate, however determined, and with what its effect is on the leaf matrix. At this stage, it may be instructive to examine the leaf matrix more closely in terms of the evaporative process and how that generates tension in the xylem phase.

The matric potential of the cell wall phase in the leaf may be considered as the sum of two inseparable components, an adsorptive and a pressure term

$$\psi_m = \psi_a + \psi_p \quad (1)$$

The meaning of Equation 1 is clarified in Figure 3 which shows a single large vertical pipe of indefinite height which narrows to capillary dimensions near the top. The system is filled with pure water to a level indicated by the meniscus in the capillary. By

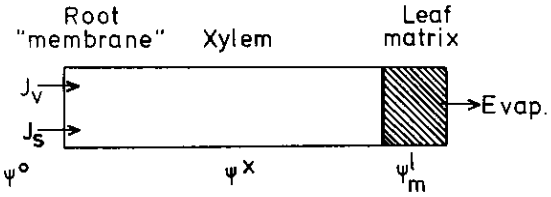

FIG. 1. Simplified plant model. Water flow through the system is driven by evaporation from the leaf matrix. J_v is the total volume flux, J_s the total solute flux, ψ^0 the external water potential, ψ^x the xylem water potential, and ψ^l_m the leaf matrix potential.

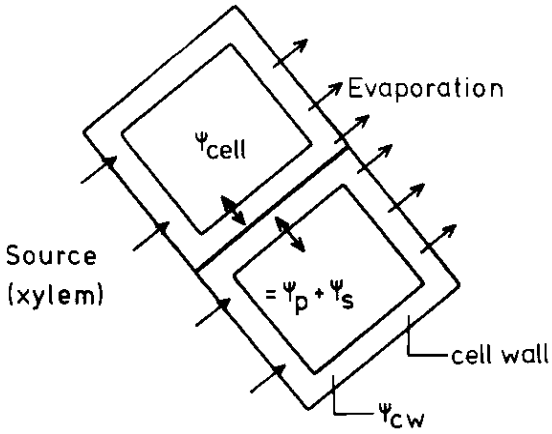

FIG. 2. Schematic representation of leaf tissue showing how absorbed water (from the source) might be partitioned between cell expansion and transpiration (evaporation).

following the dashed line vertically through the center of the system, we can examine the components of the potential arbitrarily referred to some elevation, $Z = 0$, while the whole system is at equilibrium. The gravitational potential ψ_g is dependent only on position and varies linearly with elevation (Fig. 3B). Inasmuch as the system is at equilibrium, the total potential, ψ_t, is the same at all Z along the line, and in this case $\psi_t = 0$. To fulfill the equilibrium requirements, ψ_g must be equal to and opposite in sign from the matric potential ψ_m. Note that the "gravitational gradient" of plant physiology, 0.1 bar m^{-1} of plant height, will be identified with ψ_m and not ψ_g. As we just stated, the components of ψ_m, ψ_p, and ψ_a are not physically separable but their relative magnitudes in the two distinct parts of the system may be diagrammed (Fig. 3B). In the region of the profile between the reference elevation ($Z = 0$) and Z_c, the adsorptive component ψ_a is practically nonexistent in the bulk fluid and the total matric potential is accounted for by ψ_p. At the transition from the bulk fluid to the capillary part of the system, ψ_a takes on a nonzero value because of the proximity of the wall material. In this example, ψ_a decreases stepwise but the transition could easily be made gradual by tapering the system across C. The overall result would not change, only the rate of change of ψ_a and ψ_p in the transition zone. Because the capillary is uniform, ψ_a has the same value at all elevations along the profile between Z_c and Z_m. Because ψ_t remains constant, ψ_p must increase at the transition and then resume its former rate of decrease with elevation so that ψ_m continues to balance ψ_g.

Replacing the pure water in the previous example with a solution of some arbitrary concentration will result in little difference in the potential profiles except that now the total potential will be represented by the unlabeled dashed line in Figure 3B which is also coincidental with the solute potential. The other potential components remain as they were, neglecting minor changes due to density differences and changes in adsorptivity effected by the solute.

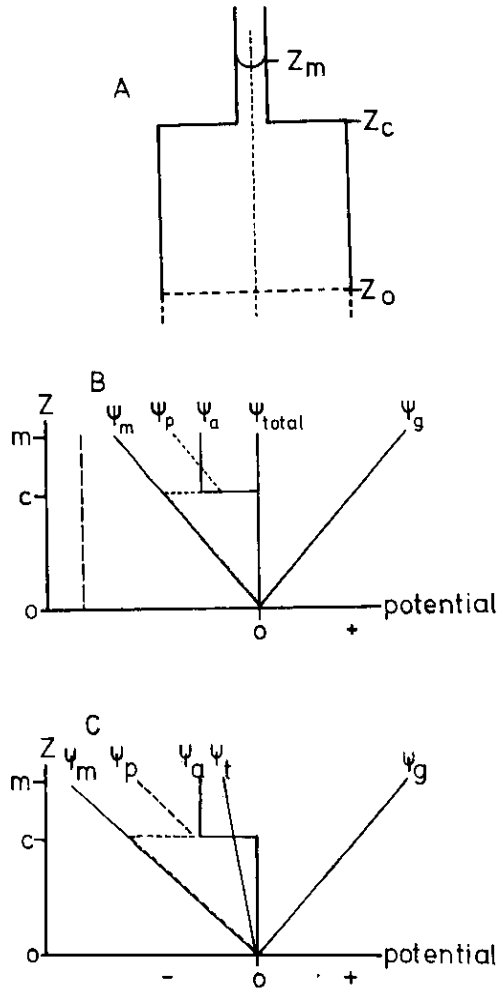

FIG. 3. A, Simple system to illustrate the transition region between the leaf matrix and the xylem. Z_0 is some arbitrary reference elevation. B, Profile of the potential components for the system in A at equilibrium. The unlabeled vertical dashed line is the total potential in the presence of solutes. C, Potential profiles for the system of A under conditions of steady state flow upwards through the system. ψ_m is leaf matric potential; ψ_p and ψ_a are the pressure and adsorptive components of ψ_m; ψ_t is total potential; ψ_g is gravitational potential.

Now consider the situation where water moves vertically through the system. Flow will be driven by evaporation from the surface of the meniscus. We would now expect the potential profiles to be modified and appear similar to Figure 3C. Evaporation from the surface tends to decrease the radius of curvature of the meniscus (see relevant comments in next paragraph), thus decreasing ψ_p and the matric potential. Since ψ_g remains unchanged, the total potential must also shift to the left (more negative), thus driving water flow. Here again, in the region $Z = 0$ to Z_c, it is the amount by which ψ_p exceeds ψ_g in magnitude which moves water. In this region ψ_a is not a factor so that ψ_m is identical to ψ_p. The major points of importance here are that the ψ_m profile is continuous through the system and that between $Z = 0$ and Z_c it may be described by ψ_p. Having established these points, we may now define a model system which can be used to describe some of the relationships between leaf water potential and volume flux through the roots.

The analogy between the system of Figure 3A and the plant is quite simple, where the capillary represents the leaf matrix and the wider part of the tube represents the xylem. Realistically, the system may be better depicted as a hollow tube topped by a finite

thickness of some fibrous matrix representing the evaporating surface (Fig. 4). The strands represent the cell wall microfibrils which are themselves made up of subunits giving each strand a somewhat porous texture of its own. The entire mat is covered with a thin film of water and the capillary menisci are located at the junctures of adjacent fibrils. Also it is much easier in Figure 4, with its tapered spaces between fibrils, to see how evaporation from the surface will result in increased curvature of the liquid surface in the interfibrillar spaces, thus leading to the reduction in ψ_p. In such a case, the microscopic view of the potential profile would have been very complex and difficult to discuss, but the major points concerning ψ_m, ψ_a, and ψ_p would be unaltered. ψ_m would still be continuous throughout the system and the cell wall matric potential in the leaves would have the same components as Equation 1.

The concept of matric potential which we are using here has its origins in the same type of adsorptive forces which are considered when many plant physiologists discuss the matric potential of cellular contents. The only difference between these two concepts is that in the case at hand the adsorptive forces are operating near a gas-liquid interface and are thus able to affect conditions in the bulk liquid by affecting the radius of curvature of the interface.

In this paper, we will deal exclusively with steady state systems in which, for the present, there is no growth of tissues and no exchange of water between the matrix and the symplasm. We will consider that the root system may be described as a semipermeable membrane with the ability to transport solutes against their potential gradient at the expense of metabolic energy. For simplicity, we will ignore frictional losses in the xylem, consider that the root membrane is possessed of ideal semipermeability so that the only solute transport is via an active mechanism (J_s^* *in mol cm*$^{-2}$ *s*$^{-1}$), and that the solutions involved behave ideally. Having established these ground rules, we can consider the simple model in Figure 1. The first task is to examine how the volume flux (J_v) through the whole system might vary as a function of the difference in potential between the leaf matrix (ψ_m^l) and the root medium (ψ^0). For steady state flow through the root membrane ($R \rightarrow X$), we may write (5)

$$J_v^R = -L^R(\psi^X - \psi^0) = -L^R(\psi_p^X - \psi_p^0 + \psi_s^X - \psi_s^0) \qquad (2)$$

where J_v^R is the volume flux density in cm^3 cm^{-2} s^{-1}, L^R is the conductance of the root membrane in cm^3 cm^{-2} s^{-1} MPa^{-1}, ψ^X is the total potential in MPa in the middle compartment (xylem), and ψ^0 is the total potential in MPa in the left hand compartment (root medium). The subscripts p and s denote pressure and solute, respectively. We can now set $\psi_p^0 = 0$ and as long as this is true drop the subscript from ψ_s^0. The van't Hoff relationship for ideal solutions gives

$$\psi_s = -RTC \qquad (3)$$

where R is the gas constant, T is the temperature in Kelvins, and

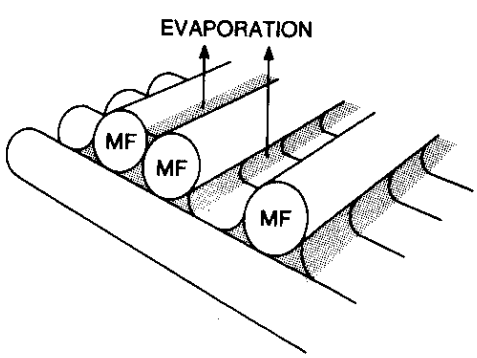

FIG. 4. Diagram of cell wall-vapor phase interface. As water evaporates the curvature of the interfacial regions increases, reducing the pressure in the liquid phase. MF, microfibrils.

C is the solute concentration in mol cm^{-3}. Volume flux through the leaf matrix from the middle compartment (xylem) to the evaporating surface may be written

$$J_v^L = -L^L(\psi^l - \psi^X) = -L^L(\psi_m^l - \psi_p^X - \psi_s^X) \qquad (4)$$

where L^L is the conductance of the matrix. Since there is no semipermeable barrier involved in this part of the system, ψ_s^X becomes irrelevant as a component of the driving force and may be eliminated from consideration. In any case, reabsorption and dilution of solutes would make any osmotic effects very minor indeed (9, 10, 14). We may now write

$$J_v^L = -L^L(\psi_m^l - \psi_p^X) \qquad (5)$$

Since we are interested in the flux response to the overall potential difference, $J_v = f(\psi_{\text{leaf}}, \psi_{\text{root medium}})$, we need to solve Equation 5 for the leaf water potential (ψ_m^l)

$$\psi_m^l = -J_v^L/L^L + \psi_p^X \qquad (6)$$

Since we are neglecting frictional losses in the xylem (see Appendix), we may now solve Equation 2 for ψ_p^X

$$\psi_p^X = -J_v^R/L^R - \psi_s^x + \psi^0 \qquad (7)$$

and substitute this into Equation 6 yielding

$$\psi_m^l = -\frac{J_v^L}{L^L} - \frac{J_v^R}{L^R} - \psi_s^X + \psi^0 \qquad (8)$$

Since $J_v^L = J_v^R$, we will use J_v for the system flux density and from Equation 3 we get $-\psi_s^X = RTC^x$. Since the membrane is ideal, C^x is a function of J_v and J_s^* only.

$$C^x = J_s^*/J_v \qquad (9)$$

Combining J_v values and making the substitution for ψ_s^x gives us

$$\psi_m^l = -J_v\left(\frac{1}{L^L} + \frac{1}{L^R}\right) + \psi^0 + \frac{RTJ_s^*}{J_v} \qquad (10)$$

For the system as a whole, we may replace the conductances with a system (equivalent) conductance, Ls, and rearrange so that the overall potential difference is

$$\psi_m^l - \psi^0 = -J_v\left(\frac{1}{L^s}\right) + \frac{RTJ_s^*}{J_v} \qquad (11)$$

Equation 11 may be rearranged to

$$J_v^2\left(\frac{1}{L^s}\right) + J_v(\psi_m^l - \psi^0) - RTJ_s^* = 0 \qquad (12)$$

and solved for J_v by the quadratic formula.

Equation 11 (the absorption function) is nonlinear in J_v for the same reasons that J_v^R is nonlinear with respect to applied pressure in excised root systems. The degree of nonlinearity will depend primarily on the magnitude of J_s^* and the ratio of the two conductances, L^L and L^R. In general, the degree and range of the nonlinearity will increase as J_s^* increases. Also, if L^L is large relative to L^R (*i.e.* the leaf matrix is more conductive than the root membrane), then the osmotic and pressure force interactions in the roots will dominate the system and the nonlinearity will be given full expression.

Under the steady state conditions we have set forth in this particular instance, it is clear that transpiration rate as well as root water flux may be expected to behave in a somewhat nonlinear manner with respect to changes in leaf water potential. This nonlinearity will of course be confounded by any absorption through the roots which goes to expansive growth rather than transpiration. In the case of steady state growth, the root water flux will be partitioned as Boyer (3) suggested between tissue expansion and transpiration.

To illustrate the effects of the water partitioning requires that we have some relationship between leaf growth and leaf water potential. Fortunately Boyer (1, 2), for example, has published data which are convenient for this purpose. Although he dealt with several species, we will confine ourselves to his data on *Helianthus* because these, better than the others, illustrate a clear maximum expansion rate. From Boyer's data, which fall from a maximum expansion rate at about −2 bars to a negligible rate at about −4 bars, we can make an initial estimate of the water-partitioning function. In this instance, we have arbitrarily chosen a sigmoid function such that

$$W_t = \frac{A - C}{1 + B(-\psi^l)^m} + C \tag{13}$$

Here, W_t is the fraction of the absorbed water which goes to transpiration, obviously between 0 and 1. A, B, C, and m are fitting coefficients which may or may not bear any quantitative relationship to physiological parameters. More will be said about this function and these coefficients in the Appendix. We can now express the transpiration rate as a function of the flux through the system and the partition function which is dependent on ψ^l.

$$T = J_v W_t \tag{14}$$

where T is the transpirational flux density, J_v is the flux density of the water reaching the evaporating site of the leaf matrix (Eq. 12), and W_t is the water partioning function (Eq. 13). Since W_t is also equal to $1 - W_g$ where W_g is the fraction of J_v going to growth, Equation 14 is a variant of Boyer's (3) partitioning function.

Now it is possible to calculate the relationship between transpiration rate and leaf water potential. To make comparisons with existing literature easier, we will express the potentials in bars and T as g dm^{-2} h^{-1} rather than in SI units. Figure 5 is an example of the kinds of curves we might expect under different conditions or looking at different parts of the plant. For example, curve A is a plot of the root water transport only (J_v^R, Eq. 2) as a function of xylem tension. Curve B, calculated from Equation 12, contains in addition the resistance of the leaf matrix and is the type of curve we would expect under steady water transport with no growth and with $\psi^0 = 0$ bar. If we now include the sigmoid partitioning function (Eq. 13), curve D results. Performing the mathematical equivalent of leaf excision, that is, removing the root transport function but supplying water to the leaf while retaining the growth partition and the leaf conductance (L^L), results in curve C.

Obviously, the choice of conductances and other coefficients will have significant effects, and discussion of these choices and some of the salient effects is in order. Having noted the shape of curve D and how it becomes coincident with curve B at high T, (*i.e.* transpiration ≅ absorption because growth is zero) and noting also from Equation 11 that T will be dominated by L^s at these high rates, it is possible to estimate L^s from Boyer's (3; Fig. 2A) data. A rough estimate of this nature gives $L^s \cong 1.04$ g dm^{-2} h^{-1} bar^{-1}. If we assume that approximately two-thirds of the system resistance resides in the roots, we can calculate L^L and L^R from L^s as 3.12 g dm^{-2} h^{-1} bar^{-1} and 1.56 g dm^{-2} h^{-1} bar^{-1}, respectively. Division by 3.6×10^5 yields, for the latter figure, 4.3×10^{-6} cm^3 cm^{-2} s^{-1} bar^{-1} which compares favorably with the range of values for root hydraulic conductances determined by Fiscus and Markhart (6). Also, these are the values which resulted in the curves of Figure 5. Curves C and D are comparable to Boyer's data from which the constants were estimated. Bear in mind, however, that he plotted ψ^l as a function of absorption and not transpiration.

Curves in the nature of Figure 5C and D may, under the proper circumstances, provide estimates of L^s and L^L. Interpretation of such data for these purposes should be done with care because of the several factors which can radically alter their shape and meaning. We will discuss each of these factors separately starting with the conductances since they (L^s at least) seem to be the easiest to estimate from these types of data. Under the conditions outlined for Figure 5, the straight line portion of the curve (D) is determined by L^s. However, the slope of this line may be altered other than by altering L^s. Examination of the water partitioning function (Fig. 6) bears on one of the initial assumptions we made concerning that partition. Considering only that fraction of water absorbed which goes to transpiration, we initially assumed this value to go from 0 to 1. There is a strong probability that this assumption is not precisely true and that at maximum growth rates there is still

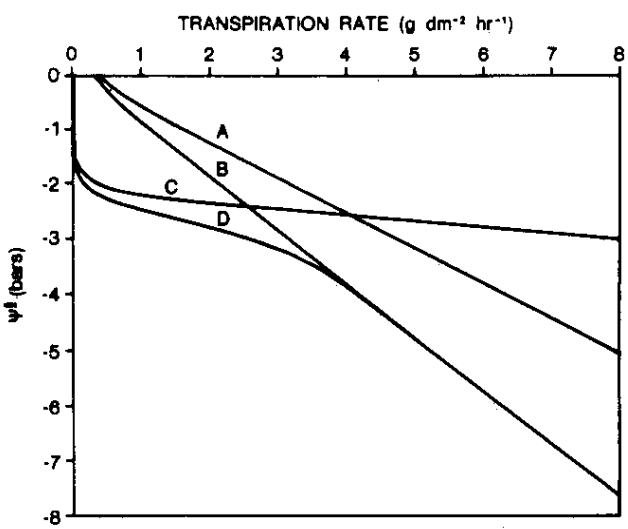

FIG. 5. Component curves for an intact plant system. A, Root water transport function (Eq. 1). B, Whole system transport function (Eq. 12). C, Excised leaf transport function with the growth partition. D, Whole system transport function with growth partition (Eq. 14). Partition function variables are the same as Figure 6, curve 1. Conductances are given in the text. $J_s^* = 3.6 \times 10^{-6}$ mol dm^{-2} h^{-1}.

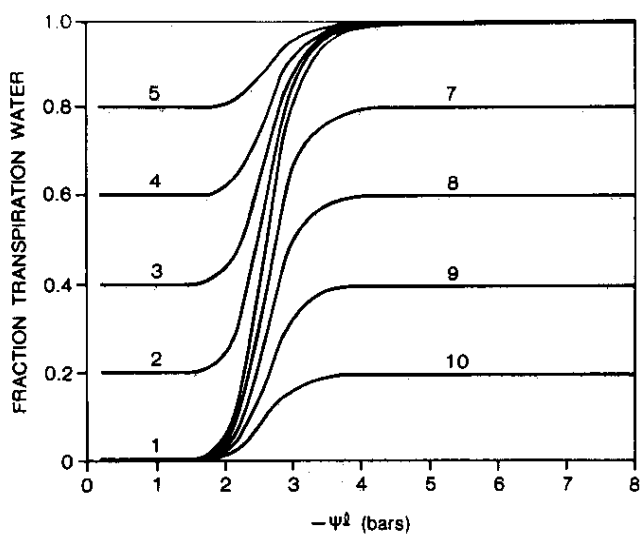

FIG. 6. Growth partition functions showing offsets at high and low leaf water potentials. Curve 1 has no offset and is calculated from Equation 13 fitted to Boyer's (1) data. For curve 1, $A = 100$, $C = 0$, $B = 22{,}471$, $m = -10.5$. Curves 2 to 5 result from various degrees of offset at high ψ^l. For example, curve 2 indicates that even during maximum growth 20% of the absorbed water is being transpired. At the other extreme, curve 10 is offset from the other direction and indicates that at low potentials (minimal growth, not zero, for this particular partition) only 20% of the absorbed water is being transpired. The offsets are produced by changing C and A in Equation 13. Curve 6 is a horizontal line coincident with the figure boundary at 1.0.

a small fraction of the water being transpired through the cuticle. The result of such cuticular transpiration would be to keep the fraction of the absorbed water going to transpiration from reaching zero at high water potentials (−2 to 0 bar). In the future, we will refer to this as the partition function "offset" at high water potentials or maximum growth rates (Fig. 6, curves 1–6). The effect of this offset is illustrated in Figure 7 where we see that the slope of the linear portion of the curve is unaffected by an offset at high growth rates. The major effect is to move the curves away from the ordinate at low T and to reduce the nonlinearity. If, for some reason, a situation develops where less than 100% of the absorbed water is transpired at any water potential, the partition functions will then be referred to as offset at low water potentials or minimum growth rates (Fig. 6, curves 7–10). In this case, one of the effects is still to reduce the nonlinearity but the slope of the linear portion of the curve is changed dramatically. It is, of course, possible for the partition functions to be offset at both ends of the potential scale, ranging, for example, from 20% to 80% of the absorbed water being transpired. Figure 8 shows the effects of such symmetrical offsets at both ends of the partition function.

Discussion of the effects of other parameters will proceed with the original 0 to 1 partition function since this seems to fit Boyer's data (3) better.

Determination of L^L could be somewhat difficult using excised leaf data (3; Fig. 2B) because the system is dominated by the partition function (Fig. 5, curve C). Examination of Figure 9 will illustrate the meaning of this statement. Figure 9 is a simulation of the excised leaf situation, as in Figure 5, curve C, where L^L is varied between 0.5 and 10 g dm^{-2} h^{-1} bar^{-1}. The salient feature of this figure is that the linear portion of the curve, that part from which L^L is estimated, becomes less and less obvious as L^L gets closer to reasonable values. By reasonable values we mean those which approximate Boyer's data (3; Fig. 2B) for excised leaves and which were estimated earlier, about 1.5 to 3.5 g dm^{-2} h^{-1} bar^{-1}. Because of the very high transpiration rates necessary to define this part of the curve for reasonable values of L^L, such an experimental determination could prove difficult.

Another major factor which could alter the shapes of the ψ^l:T curves is the water potential of the soil or solution (ψ^0) surrounding the roots. The effect of lowering ψ^0 is shown in Figure 10. The system conductance (L^s) in this case is not changed, but the shapes of the curves would be altered as the partition function, which

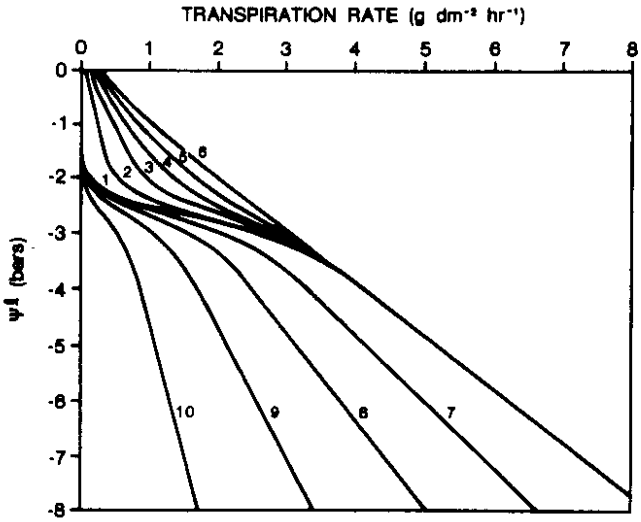

FIG. 7. Effect of growth partition offsets (Fig. 6) on the form of the T:ψ^l curve. Numbers on the curves correspond to the numbers on the partition functions of Figure 6. Curve 6 is the case where there is no growth partition (*i.e.* a 100% offset in Fig. 6). Plant parameters are the same as curve D, Figure 5.

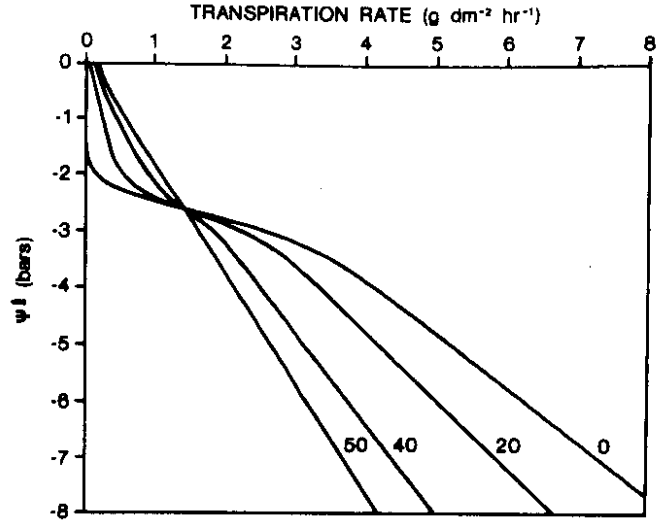

FIG. 8. Effect of symmetrical offsets of the partition function at high and low potentials. For example, curve 20 results from a growth partition function where 20% of the absorbed water is transpired at high potentials and only 80% is transpired at low potentials. Plant parameters are the same as curve D, Figure 5.

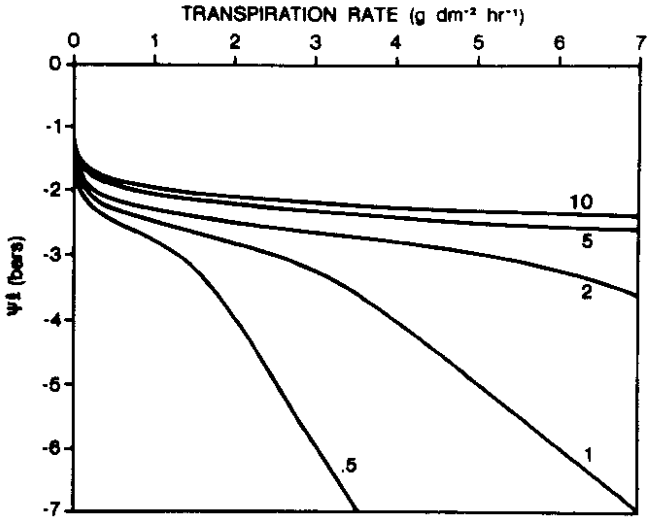

FIG. 9. Effect of L^L on the excised leaf T:ψ^l relationship showing the problems of determining L^L from data of this type for "reasonable" values of L^L. Numbers on curves are L^L in g dm^{-2} h^{-1} bar^{-1}.

dominates at high ψ^0, is gradually swamped out by the inhibitory effects of lowered ψ^0. That is, growth is slowed and successively smaller portions of the curve are influenced by growth. In this particular instance for ψ^0 at around −4 to −5 bars, the curves become identical with those which would result if there were no partition function (absorption = transpiration). One would also expect this same effect if the effective external potential were lower than indicated by measurement of the bulk soil or solution due to buildup of solutes at the root surface or complications from an intermediate root compartment (5) or localized soil drying at the root surface. Soil conductivity decreases associated with drying soils can also be expected to exaggerate these effects and to shift the curves toward steeper slopes.

Another phenomenon which may cause the linear portions of the slope to steepen is breakage of the water columns in the xylem under conditions of a high energy load on the leaves or drying soil or both. If the breakage is extensive enough, it may result in a reduction of L^s. Clearly, reductions in L^s along with a drying soil would make quantitative interpretations of the data more

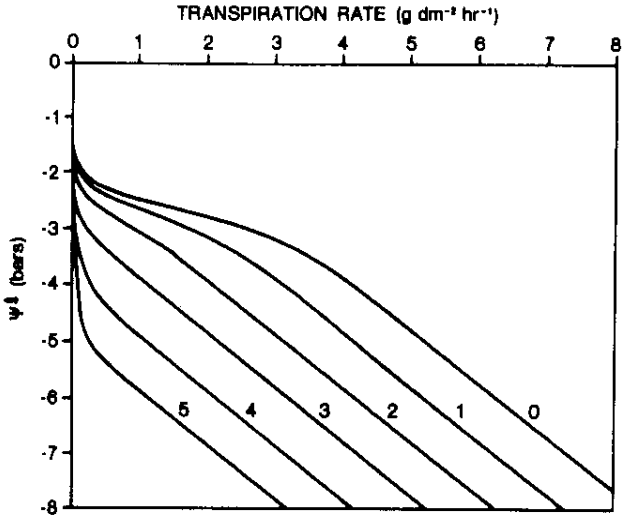

FIG. 10. Effect of root medium water potential on the T:ψ^l relationships. Numbers on curves are $-\psi^0$; all other parameters are the same as for Figure 5. Note that curve 5 is identical to that resulting from no growth partition.

difficult. For example, we can assume that the xylem cavitates sufficiently to reduce L^s at $\psi^l = -6$ bars. We could then expect all of the curves in Figure 10 to break again (steepen vertically) at around −6 bars. More likely, cavitation would proceed over a range of potential values and the curves would reflect the gradual reduction in L^s so that we may never see a linear portion for the curves of interest.

In general, the plateau (most nearly horizontal) portions of the curves, particularly for the excised leaves, are dominated by the partition function, especially the steepness of the transition between maximum growth and no growth. If this transition is very sharp, then the plateau may approach the horizontal and accurate determinations of the slope would require very precise determinations of leaf and soil water potentials, a matter that can present substantial experimental difficulties. Obviously, the water potential at which growth begins to decline will influence the position of the plateau region on the ordinate.

Leaf expansion generally will not proceed at a steady rate indefinitely. Therefore, the partition function may vary with time depending upon cell wall extensibility and osmotic adjustment phenomena. Because of this, it should be possible to obtain experimental data, on the same leaf, resembling curves B or D of Figure 5 or any intermediate depending upon the particular timing of the experiment. This shift in the growth-related partition function may have some bearing on the interpretation of the data of Bunce (4) who observed shifting relationships between ψ^l and T depending on how long he waited to make his measurements after achieving steady state transpiration.

Longer term changes in the partition function will also cause shifts in the T:ψ^l relationships. Such changes should be observable in individual leaves as they undergo growth, maturation, and senescence. Seasonal changes in perennial as well as annual plants may also be expected to alter the water partition function, thus, the T:ψ^l relationships.

In addition, the ψ^l:T curves compiled by Hailey *et al.* (7) and by Kaufmann (8) might be explained according to differing growth partition functions, conductances (L^s), ψ^0, and the portion of the curve where the data were obtained.

The horizontal portions of the curves for herbaceous plants are not difficult to explain conceptually but would require a very sharp cutoff of growth. Judging from Boyer's data for corn and soybean (2), however, this situation may not be at all unusual, particularly for plants grown under growth chamber conditions. His data indicate a nearly vertical transition of ψ^l between maximum and minimum growth rate over a large part of the range of growth rates. The length of the horizontal part of the curve will depend upon over what portion of the growth range the vertical transition extends. In addition, lowering ψ^0 can eliminate the plateau region entirely (Fig. 10) as can lowering the conductance (Fig. 9).

The relationships between ψ^l and T of woody plants also appears to be explained readily by the proposed model. A marked difference between woody and herbaceous plants is that leaf water potentials in woody plants are rarely less negative than −3 or −4 bars, while herbaceous plants frequently have potentials much closer to zero (8). To our knowledge, no reports exist for woody plants of the response type shown in curve B, Figure 5, where water potentials of zero are shown which are the result of root pressure phenomena. Root pressure activity in trees is much less common than in herbaceous plants (11) and reports of root pressure activity in conifers are less common still (12, 15–17, 19). Even so, it has been perplexing that potentials closer to zero have not been observed even with plants enclosed in a dark, humid chamber (8).

Woody plants frequently have ψ^l:T relationships similar to curve D, Figure 5, at the lower transpiration rates (8). While leaf growth may not be occurring, it is entirely possible that growth of other tissues (*i.e.* cambial activity or root growth) has existed during most of the studies reported. Perhaps growth of these tissues results in decreased leaf water potentials at zero transpiration as a direct consequence of water partitioning. There appears to be no reason that the growth sink for water must be located very close to the evaporating sites in the leaf.

Interpretation of the leaf matrix conductance L^L is not clear. Our development has assumed this to include the petiole resistance, if not completely negligible, as well as any other structures over, between, or through which water must pass to reach the evaporating surface of the leaf tissues. Therefore, readers' interpretation will depend upon the precise pathway they particularly favor. It does seem clear, however, that water evaporates from the wall matrix of those cells suitably situated and that the potential of this matrix is the major factor controlling water flux into the leaf during transpiration. The potential of this matrix is presented to the protoplasts, and it is this potential which is measured (at least attempted) with vapor equilibrium (psychometric) techniques whether *in situ* or in excised samples.

There are several conditions under which the absorption function (Eq. 11) will interact with or dominate the partition function and so control the shape of the ψ^l:T relationship. In the first case, where growth is slowed considerably or stopped entirely, the absorption function will define the shape of the curve. The second case occurs when ψ^0 becomes significant relative to the leaf water potential where expansive growth begins to slow. Throughout this paper, except for Figure 10, we have set $\psi^0 = 0$ so that this should not have been a growth-inhibiting factor. However, some of Boyer's (2) data for corn and soybean indicate that growth inhibition may begin at potentials as high as −1 bar. Third, decreases in L^s as, for example, brought about by lowering the root temperature leading to decreased L^R will allow the absorption function to dominate the system. Estimates of changes in root conductance from the data of Markhart *et al.* (13) indicate that lowering the root temperature will reduce L^R in soybeans at 15°C to about one-third of its value at 25°C. In growing plants, the range of ψ^l over which growth occurs will be traversed over a much narrower range of transpiration rates. For comparison, the curves labeled 1 and 0.5 in Figure 9 will give an indication of the effect of reducing L^R by half (less than a 10°C decrease). In nongrowing plants, the salient effects will be to steepen the slope of the line and reduce the intercept (Fig. 5, curve B).

So far in this paper, we have made no attempt to deal with the

limitations imposed on the system by stomatal closure and have dealt with water transport within the plant as though it were transpiring at its potential rate under any set of circumstances. Since most of the simulations and data cited in this paper cover a narrow range of high water potentials, it is unlikely in these circumstances that stomatal responses would impose serious limitations on the system. However, it is easy to see that the effect of stomatal closure might be to cut off the portion of the curve below potentials which close the stomata. Because stomatal responses to ψ^l can be sluggish, it is more likely that a loop of some sort would be set up on the curve near the operating point of the stomata. Over greater portions of the curve, nonsteady state changes in the water content of larger plants, due to movement into and out of the xylem, may alter the supply of water available for evaporation and introduce a major hysteresis loop into the ψ^l:T relationship.

One obvious conclusion to be drawn from this paper is that the circumstances under which we should expect a truly linear relationship, passing through the origin, between ψ^l and T, are really much more rare than would be the opposite expectation. The primary reasons for the overall nonlinearities are the nonlinearity in the root absorption function (5) and the partitioning of the absorbed water between growth and transpiration (3). The relative importance of these two in determining the shape of the ψ^l:T curve depends mostly on the system conductance, the root medium water potential, and the shape of the partition function.

Another philosophical point to be made, from an instructive point of view, is that the relationships dealing with bulk fluid flow, diffusion, and solute transport are as adequate for describing the system as are any analogically based equations. Therefore, perhaps we should abandon the Ohm's law analogy as a means of both instructing students and expressing our research data, if for no other reason than the level of expectation of linearity which is inherent in many physiological interpretations of Ohm's law.

This paper suggests fairly direct means for determining L^s from the linear portions of the curve, provides some insight into the growth partitioning function, and points out various circumstances which must prevail for the proper interpretation of the data. It appears that a relatively simple model of water flow accounts for the major features of water transport in both herbaceous and woody plants.

LITERATURE CITED

1. Boyer JS 1968 Relationship of water potential to growth of leaves. Plant Physiol 43: 1056–1062
2. Boyer JS 1970 Leaf enlargement and metabolic rates in corn, soybean, and sunflower at various leaf water potentials. Plant Physiol 46: 233–235
3. Boyer JS 1974 Water transport in plants: mechanism of apparent changes in resistance during absorption. Planta 117: 187–207
4. Bunce JA 1978 Effects of shoot environment on apparent root resistance to water flow in whole soybean and cotton plants. J Exp Bot 29: 595–601
5. Fiscus EL 1977 Determination of hydraulic and osmotic properties of soybean root systems. Plant Physiol 59: 1013–1020
6. Fiscus EL, AH Markhart III 1979 Relationships between root system water transport properties and plant size in *Phaseolus*. Plant Physiol 64: 770–773
7. Hailey JL, EA Hiler, WR Jordan, CHM Van Bavel 1973 Resistance to water flow in *Vigna sinensis* L. (Endl.) at high rates of transpiration. Crop Sci 13: 264–267
8. Kaufmann MR 1976 Water transport through plants: current perspectives. *In* IF Wardlaw, JB Passioura, eds, Transport and Transfer Processes in Plants. Academic Press, New York, pp 313–327
9. Klepper B 1967 Effects of osmotic pressure on exudation from corn roots. Aust J Biol Sci 20: 723–735
10. Klepper B, MR Kaufmann 1966 Removal of salt from xylem sap by leaves and stems of guttating plants. Plant Physiol 41: 1743–1747
11. Kramer PJ, TT Kozlowski 1979 Physiology of Woody Plants. Academic Press, New York, p 453
12. Lopushinsky W 1980 Occurrence of root-pressure exudation in Pacific Northwest conifer seedlings. For Sci 26: 275–279
13. Markhart III AH, EL Fiscus, AW Naylor, PJ Kramer 1979 Effect of temperature on water and ion transport in soybean and broccoli systems. Plant Physiol 64: 83–87
14. Oertli JJ 1966 Active water transport in plants. Physiol Plant 19: 809–817
15. O'Leary JW 1965 Root pressure exudation in woody plants. Bot Gaz 126: 108–115
16. O'Leary JW, PJ Kramer 1964 Root pressure in conifers. Science 145: 284–285
17. Sands R, EL Fiscus, CPP Reid 1982 Hydraulic properties of pine and bean roots with varying degrees of suberization, vascular differentiation, and mycorrhizal infection. Aust J Plant Physiol 9: 559–569
18. Spain JD 1982 BASIC Microcomputer Models in Biology. Addison Wesley, Reading, MA, p 51
19. White PR, E Schuker, JR Kern, FH Fuller 1958 Root pressure in gymnosperms. Science 128: 308–309

APPENDIX

Root Area/Leaf Area. The development of the arguments in this paper assumes that the leaf and root areas are the same so that the flux density to the evaporating surface of the leaves is the same as the flux density through the roots. For other root:leaf area ratios the mass balance requirement is that the total fluxes through the root system and to the evaporating surface of the leaves be equal. If Q_R and Q_L are the total root flux and total leaf flux respectively in $cm^3\ s^{-1}$, then the relationships between the Q and J_v values are

$$Q_R = A^R J_v^R \text{ and } Q_L = A^L J_v^L \tag{15}$$

where A^R and A^L are root and leaf areas, respectively. At the steady state, $Q_R = Q_L = Q$. Following the development (Eqs. 2–11) in the same fashion as before leads to

$$\psi_m^l - \psi^0 = -Q\left(\frac{1}{A^L L^L} + \frac{1}{A^R L^R}\right) + \frac{A^R RTJ_s^*}{Q} \tag{16}$$

which is similar in form and purpose to Equation 11 except that differences in the relevant surface areas are accounted. In addition, Equation 14 now becomes

$$T = (Q/A^L)\ W_t \tag{17}$$

Xylem Transport. In situations where the xylem resistance for one reason or another cannot be considered negligible, the pressure losses in the xylem may be treated by the Poiseuille equation or whatever other form the reader finds most satisfactory. First, the pressure (or tension) loss in the xylem may be written as

$$\psi_p^{XL} - \psi_p^{XR} = -Q\frac{8\eta\Delta x}{\Pi\Sigma r^4} \tag{18}$$

where η is the viscosity of the fluid, Δx the length of the xylem, and r the radius of the individual xylem elements and Q is the flow rate (17). The superscripts XL and XR refer to the xylem at the leaf and root ends, respectively.

The leaf water potential is now written as

$$\psi_m^l = -\frac{Q_L}{A^L L^L} + \psi_p^{XL} \tag{19}$$

Similar to Equation 7, the xylem tension at the root end may be written

$$\psi_p^{XR} = -\frac{Q_R}{A^R L^R} + \psi^0 - \psi_s^x \tag{20}$$

Solving Equation 18 for ψ_p^{XL} and substituting in Equation 19, and substituting Equation 20 in that result, yields at the steady state

$$\psi_m^l - \psi^0 = -Q\left(\frac{1}{A^L L^L} + \frac{1}{A^R L^R} + \frac{8\eta\Delta x}{\Pi\Sigma r^4}\right) + \frac{A^R RTJ_s^*}{Q} \tag{21}$$

Again, Equation 17 describes the transpiration rate.

It should be noted here that the effect of adding the xylem resistance term to the system would have the same effect on the leaf potential/transpiration curve as decreasing either the root, leaf, or system conductances (see Fig. 9).

Partition Function. Equation 13 describes the way the absorbed water is divided between growth and transpiration. Reference to

Figure 6 will help to clarify the influence of the various coefficients in Equation 13. Interaction between the coefficients B and m is complex, but together they act to fix the position of the transitional (vertical) part of the curve and the steepness of the transition. Initial estimates of B and m may be obtained by regression of the linear transform given in Spain (18). The various offsets discussed in the text are produced by manipulating A and C. Coefficients A and C set the partition limits (offsets) for high and low values, respectively, of the independent variable ($-\psi^l$). For example, for curve 1 in Figure 6, $A = 1$ and $C = 0$; for curve 2, $A = 1$ and $C = 0.2$; and for curve 7, $A = 0.8$ and $C = 0$. Combinations of offsets other than those shown may be produced by setting A and C to whatever values are desired. Mathematically, it is not even necessary that $A > C$, so it is possible to produce a curve ranging from 1 to 0, with increasing absolute value of ψ^l, simply by setting $A = 0$ and $C = 1$.